Development 140, 1475-1485 (2013) doi:10.1242/dev.087601

Coronary veins determine the pattern of sympathetic innervation in the developing heart

Joseph Nam[1,*], Izumi Onitsuka[1,*], John Hatch[1,*], Yutaka Uchida[1], Saugata Ray[2], Siyi Huang[3], Wenling Li[1], Heesuk Zang[1], Pilar Ruiz-Lozano[2,4] and Yoh-suke Mukouyama[1,‡]

SUMMARY

Anatomical congruence of peripheral nerves and blood vessels is well recognized in a variety of tissues. Their physical proximity and similar branching patterns suggest that the development of these networks might be a coordinated process. Here we show that large diameter coronary veins serve as an intermediate template for distal sympathetic axon extension in the subepicardial layer of the dorsal ventricular wall of the developing mouse heart. Vascular smooth muscle cells (VSMCs) associate with large diameter veins during angiogenesis. *In vivo* and *in vitro* experiments demonstrate that these cells mediate extension of sympathetic axons via nerve growth factor (NGF). This association enables topological targeting of axons to final targets such as large diameter coronary arteries in the deeper myocardial layer. As axons extend along veins, arterial VSMCs begin to secrete NGF, which allows axons to reach target cells. We propose a sequential mechanism in which initial axon extension in the subepicardium is governed by transient NGF expression by VSMCs as they are recruited to coronary veins; subsequently, VSMCs in the myocardium begin to express NGF as they are recruited by remodeling arteries, attracting axons toward their final targets. The proposed mechanism underlies a distinct, stereotypical pattern of autonomic innervation that is adapted to the complex tissue structure and physiology of the heart.

KEY WORDS: NGF, Cardiac innervation, Coronary development, Sympathetic axons, Vascular smooth muscle

INTRODUCTION

Cardiac tissues are highly vascularized and extensively innervated by autonomic nerves. Abnormal patterning and distribution of the coronary vasculature is often associated with congenital heart disease (Kayalar et al., 2009), while impairment of autonomic functions can lead to lethal arrhythmia (Hildreth et al., 2009). Previous studies have shown neurovascular interactions in other tissues to be crucial in the development of both nerves and vasculature (reviewed by Carmeliet and Tessier-Lavigne, 2005; Larrivée et al., 2009). The importance of these structures in cardiac development and homeostasis led us to examine the possibility of coordinated development in the murine heart.

Coronary vasculature develops from an existing primary capillary plexus via a remodeling process known as angiogenesis (reviewed by Lavine and Ornitz, 2009). During angiogenic remodeling, endothelial cells reorganize to form a hierarchical branching network, and larger vessels recruit vascular smooth muscle cells (VSMCs). Recent studies in mice have revealed that large diameter coronary veins develop close to the epicardial surface layer (the subepicardium), whereas coronary arteries arise separately in the deeper myocardial layer (Lavine et al., 2008; Red-Horse et al., 2010). Early studies in avian and murine models demonstrated that the epicardium, which is derived from the proepicardium, an extracardiac rudimentary organ, gives rise to coronary VSMCs and provides pro-angiogenic factors such as fibroblast growth factors (FGFs) and vascular endothelial growth factors (VEGFs) (reviewed by Lavine and Ornitz, 2009).

Sympathetic innervation of the heart originates in the stellate ganglia. Previous studies have shown that arterial VSMCs mediate proximal sympathetic axon extension by secretion of artemin (Enomoto et al., 2001; Honma et al., 2002), neurotrophin 3 (Francis et al., 1999; Kuruvilla et al., 2004) and endothelins (Makita et al., 2008). Although proximal extension out of the ganglia is well characterized, the mechanisms responsible for distal extension to reach target cells remain elusive. In distal axon extension, nerves adopt a stereotypical pattern in target tissues prior to innervating final target cells. Nerve growth factor (NGF) is required for terminal sympathetic innervation of target tissues (Glebova and Ginty, 2004). Mutants lacking *Ngf* and Bcl2-associated X protein (*Bax*) have normal sympathetic axon extension along the extracardiac vasculature but sympathetic innervation is drastically decreased in the heart. This concomitant knockout of the pro-apoptotic factor *Bax* allows neurons to survive in the absence of NGF, demonstrating that NGF plays a role in distal cardiac sympathetic axon growth that is distinct from its role in survival (Glebova and Ginty, 2004). However, the precise origin and function of NGF during cardiac innervation remain to be examined.

We found anatomical congruence between nerves and coronary vessels in the developing heart. Beginning at embryonic day (E) 13.5, sympathetic axons extend along developing large diameter coronary veins in the dorsal subepicardium of the ventricles. By E15.5, these axons extend across the entire dorsal surface and subsequently penetrate the dorsal myocardium while others begin to reach the ventral subepicardium. Mutant analyses indicate that this neurovascular association is important for proper cardiac innervation but not for coronary vascular patterning. *In vitro* and *in*

[1]Laboratory of Stem Cell and Neuro-Vascular Biology, Genetics and Developmental Biology Center, National Heart, Lung, and Blood Institute, National Institutes of Health, Building 10/6C103, 10 Center Drive, Bethesda, MD 20892, USA. [2]Development and Aging Program, Sanford-Burnham Medical Research Institute, 10901 North Torrey Pines Road, La Jolla, CA 92037, USA. [3]Department of Neuroscience, The Johns Hopkins University School of Medicine, 725 North Wolfe Street, Baltimore, MD 21205, USA. [4]Pediatric Cardiology, Stanford University School of Medicine, 300 Pasteur Drive, Palo Alto, CA 94305, USA.

*These authors contributed equally to this work
‡Author for correspondence (mukoyamay@mail.nih.gov)

Accepted 25 January 2013

vivo experiments further demonstrate that epicardium-derived venous VSMCs direct the extension of sympathetic axons via secretion of NGF during their recruitment to coronary veins. As venous remodeling completes, subepicardial VSMCs downregulate NGF expression. Subsequently, myocardial VSMCs begin to express NGF during arterial remodeling, stimulating axon extension towards final target cells in that layer. Our data suggest a model in which large diameter coronary veins serve as an intermediate template for sympathetic axon outgrowth. This template appears to ensure a proper distribution of sympathetic axons for eventual innervation of target cells in the myocardium. At the molecular level, sequential expression of NGF in subepicardial venous VSMCs and myocardial arterial VSMCs is responsible for a two-step process of distal axon extension and subsequent innervation of myocardial arteries.

MATERIALS AND METHODS

Experimental animals

Characterization of *ephrinB2*$^{taulacZ/+}$ (Wang et al., 1998), *EphB4*$^{taulacZ/+}$ (Gerety et al., 1999), *ChAT*^{BAC}*-eGFP* (Tallini et al., 2006), *SM22α*$^{lacZ/+}$ (Zhang et al., 2001; Walker et al., 2005), *Phox2b*$^{-/-}$ (Pattyn et al., 1999) and *Gata5-Cre; β-catenin*$^{flox/flox}$ (Zamora et al., 2007) mice has been reported elsewhere. *NGF*$^{lacZ/+}$ knock-in mice were generated in David Ginty's laboratory at Johns Hopkins University by homologous recombination in ES cells according to standard procedures. All experiments were carried out according to the guidelines approved by the Animal Care and Use Committee at NHLBI.

Whole-mount immunohistochemistry of embryonic hearts

Whole-mount immunohistochemical staining of embryonic hearts was performed essentially as described previously (Mukouyama et al., 2002). Embryonic hearts were dissected and fixed in 4% paraformaldehyde/PBS overnight at 4°C. The antibodies used were: anti-PECAM1 (clone MEC13.3, BD Pharmingen, 1:300) to detect endothelial cells; anti-SM22α (Abcam, 1:250) and Cy3-conjugated anti-αSMA (clone 1A4, Sigma, 1:500) to detect VSMCs; anti-β-tubulin (βIII) (clone TuJ1, Covance, 1:500) to detect nerve fibers; anti-CGRP (Millipore, 1:500~1000) to detect sensory neurons; anti-TH (Novus Biologicals, 1:500~1000) to detect sympathetic neurons; and anti-β-galactosidase (MP Biomedicals, 1:5000) to detect *lacZ* expression. Different combinations of Alexa 488-, Alexa 568-, Cy3- or Dylight 649-conjugated secondary antibodies (Invitrogen or Jackson, 1:250) were used for staining. Confocal microscopy analysis was carried out on a Leica TCS SP5 confocal microscope.

Section immunohistochemistry

Fresh embryos were embedded in OCT compound (Sakura), followed by cryosectioning into 6-8 μm sections and collected on precleaned slides (Matsunami, Japan). Staining was performed using the following antibodies: anti-NGF (Millipore, 1:200); anti-ARTN (R&D, 1:250); anti-β-gal (1:5000); anti-EDN1 (Abbiotec, 1:250); anti-GMFβ (ProteinTech, 1:100); anti-GMFγ (ProteinTech, 1:250); anti-NRG1 (R&D, 1:250); anti-PECAM1 (1:300); anti-SM22α (1:250) and Cy3-conjugated anti-αSMA (1:500). For immunofluorescence detection, Alexa 488-, Alexa 568-, Cy3- or Dylight 649-conjugated secondary antibodies (Invitrogen or Jackson, 1:250) were used.

RNA *in situ* hybridization analysis

In situ hybridization analysis was performed as described previously (Wang et al., 1998). The probes were amplified using the primers listed in supplementary material Table S1. The hybridization signal was detected using an alkaline phosphatase-conjugated anti-digoxigenin antibody and BCIP/NTB (Roche).

RT-PCR analysis

Total RNA was purified from tissues and cultured cells using Trizol Reagent (Invitrogen) followed by reverse transcription into first-strand cDNA using the SuperScript III First-Strand Synthesis Supermix kit (Invitrogen) according to the manufacturer's instruction. Quantitative mRNA expression analysis of chemokines and their receptors in E13.5 dorsal root ganglia and forelimbs was performed with the Mouse Chemokine and Receptor RT^2 Profiler PCR Array (Qiagen) on a 7500 real-time PCR system (Applied Biosystems) using RT^2 SYBR Green qPCR Master Mix (Qiagen). The results of mRNA expression of *Ngf*, *Artn*, *Edn1*, *Gmfb*, *Gmfg* and *Nrg1* were confirmed by semi-quantitative RT-PCR (supplementary material Table S1).

Preparation of coronary VSMCs from primary fetal epicardial culture

Primary fetal epicardial cells were obtained as a source of coronary VSMCs (Rhee et al., 2009). Heart ventricles were dissected from E12.5 or E13.5 embryos and cultured in 1% collagen type I gel (rat tail collagen, BD) containing αMEM (Invitrogen), 10% FBS (Hyclone), 10 ng/ml bFGF (FGF2; NCI BRB Preclinical Repository) and 10 ng/ml EGF (PeproTech). The ventricles were removed from the gel, and migrated epicardial cells were harvested with a 0.1% collagenase treatment. Isolated epicardial cells were further cultured on a type IV collagen-coated dish (BD) with 10% FBS in DMEM (Invitrogen) containing 10 ng/ml bFGF and 10 ng/ml EGF. Epicardial cells differentiated to VSMCs in response to serum and/or 50 ng/ml TGFβ1 (PeproTech). Some cultures were infected with *Ngf* or control shRNA lentiviruses (3×10^5 transducing units shRNA lentivirus particles for 1×10^5 VSMCs; Sigma). The effect of shRNA knockdown was confirmed by RT-PCR analysis. To generate a VSMC aggregation for co-culture with sympathetic ganglia explants, a hanging drop culture method was used.

Primary sympathetic ganglia explant co-culture and staining

Sympathetic ganglia (SG) were dissected from E13.5 embryos and cultured on 1% collagen type I gel (Makita et al., 2008). SG were then cultured on 1% collagen type I gel containing αMEM, 10% FBS and 0.3% sodium bicarbonate (Invitrogen). Some SG explant cultures were supplemented with 20 ng/ml ARTN (R&D), 100 ng/ml EDN1 (R&D), 20-100 ng/ml GMFβ (PeproTech), 20-100 ng/ml GMFγ (PeproTech), 25 ng/ml NGF (Upstate) and 100 ng/ml NRG1 (R&D). NGF- (2.5 μg/ml in PBS) or PBS-soaked heparin-agarose beads (Bio-Rad) were placed next to SG explants. Cultures were incubated in the CO_2 incubator for 2 days. For co-culture with VSMCs, SG explants were placed next to VSMC aggregations on 1% collagen type I gel. Some co-cultures were treated with the neutralizing antibodies 10 μg/ml anti-ARTN (R&D), 200 ng/ml anti-NGF (R&D) or 20 μg/ml anti-NRG1 (R&D) and EDN1 receptor-selective antagonists (2 μM BQ123 and 200 nM BQ788, Sigma). We established that each inhibitor successfully blocks the effect of its factor on SG explants. Fetal epicardial and myocardial tissues were dissected from the cardiac ventricles of E13.5 or E16.5 embryos. Both tissues were independently cultured with SG explants on 1% collagen type I gel. Staining was performed using anti-SM22α antibody, αSMA antibody, or anti-TUJ1 antibody in combination with the pan-nuclear marker To-Pro-3 (Invitrogen). Volocity software (PerkinElmer) was used to quantify axon outgrowth from confocal images of TUJ1$^+$ SG axons in the co-culture experiments. SG explants were divided into four quadrants (see Fig. 6F), intersecting at the center of the explant. Axon outgrowth was quantified by comparing total axon length and number of projections between the quadrants facing and opposite the VSMC aggregates or myocardium. Statistical significance was assessed using Student's *t*-test.

In ovo implantation

Heparin-agarose beads (Bio-Rad) were soaked for 3 hours in 10 μg/ml isotype IgG or NGF-neutralizing antibody (R&D) or in 2.5 μg/ml NGF or BSA. The beads were implanted on the dorsal surface of E6 chick hearts. Chick embryos were harvested at E10 and the hearts were immunostained with anti-αSMA antibody and anti-TUJ1 antibody in whole-mount.

RESULTS

Cardiac sympathetic axons associate with large diameter coronary veins within the subepicardium

In order to examine the anatomical architecture of cardiac nerves and coronary vasculature, we developed a whole-mount immunohistochemistry method for the mouse embryonic heart.

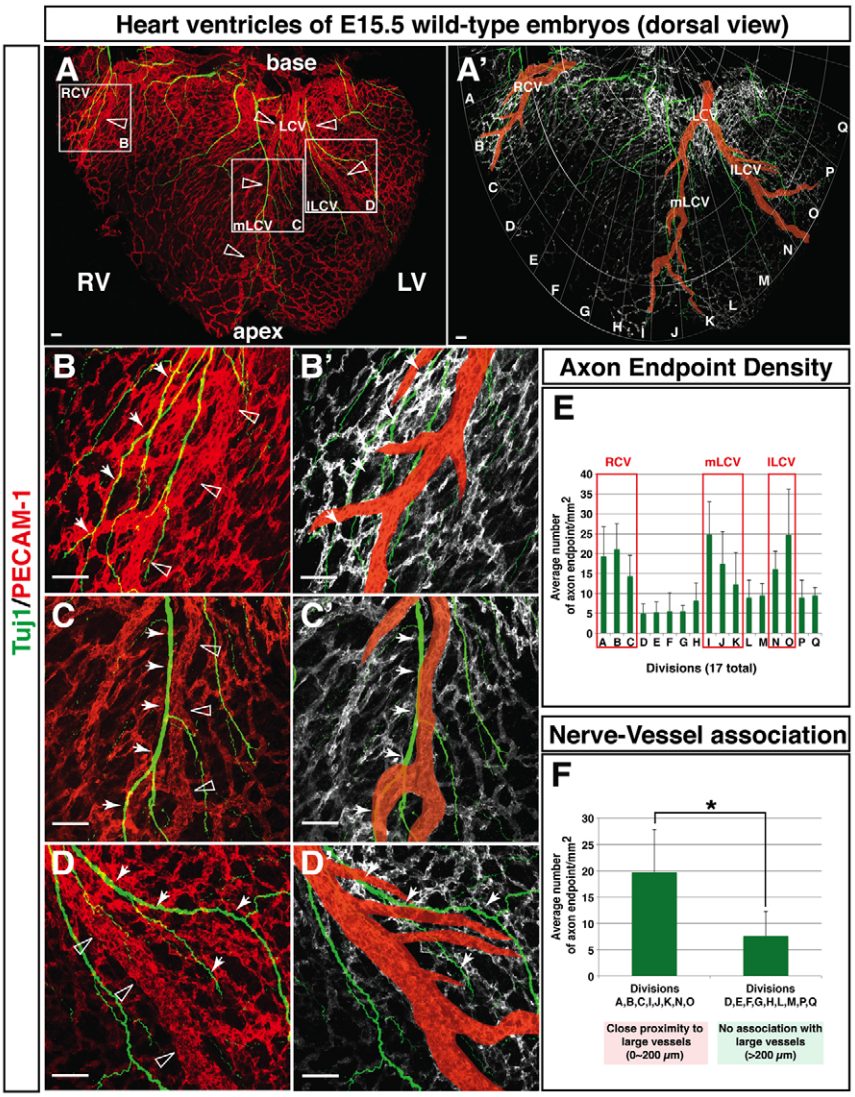

Fig. 1. Cardiac nerves align with large diameter coronary vessels in the dorsal ventricular wall of the developing heart. (**A-D′**) The dorsal face of the cardiac ventricles of an E15.5 mouse embryo. Whole-mount double immunofluorescence confocal microscopy using antibodies to the pan-endothelial marker PECAM1 (A-D, red; A′-D′, white) and the neuronal marker class III β-tubulin (TUJ1, green) reveals that TUJ1$^+$ cardiac axons (A,A′) follow three remodeled large diameter coronary vessels: the right cardiac vein (RCV), the medial branch of left cardiac vein (mLCV), and the lateral branch of left cardiac vein (lLCV) (A, open arrowheads; A′, pseudocolored in red). Magnified images (B-D′) of the boxed regions in A clearly demonstrate the physical proximity of TUJ1$^+$ cardiac axons (B-D′, arrows) and large diameter vessels (B-D, open arrowheads; B′-D′, pseudocolored in red). (**E**,**F**) Quantification of nerve-vessel association. In 17 radial sections of the dorsal ventricular wall (termed A-Q, see A′), axons most commonly project to regions containing RCV, mLCV or lLCV. *P<0.01 (Student's t-test); n=7; error bars indicate s.e.m. RV, right ventricle; LV, left ventricle. Scale bars: 100 μm.

Double staining with antibodies specific for PECAM1, a pan-endothelial cell marker, and the neuronal marker class III β-tubulin (TUJ1) revealed the structure of coronary vasculature and the extent of cardiac innervation at E15.5 (Fig. 1A). Three large diameter vascular branches (25-100 μm) were apparent in the subepicardial layer of the dorsal wall of the ventricles: the right cardiac vein (RCV), the medial branch of the left cardiac vein (mLCV), and the lateral branch of the left cardiac vein (lLCV) [Fig. 1A′; as referred to by Ciszek et al. (Ciszek et al., 2007)]. All three vessels associated with TUJ1$^+$ axons (Fig. 1A,A′). Notably, magnified images showed large diameter vessels and axons in close proximity (0-200 μm) with strikingly similar branching patterns (Fig. 1B-D′). We quantified the extent of nerve-vessel association: the dorsal surface of the ventricles was divided into 17 radial sections (termed A-Q). In each section, the relative axon density was calculated (number of axon end points/surface area; Fig. 1E). The quantification revealed that axons are significantly more likely to project to regions near large diameter vessels (Fig. 1F).

We further characterized the structures found in our initial staining. *EphB4*$^{taulacZ/+}$ embryos allowed us to visualize the venous marker EPHB4, while *ephrinB2*$^{taulacZ/+}$ embryos were used to image the arterial marker ephrin B2 (Wang et al., 1998; Gerety et al., 1999; Mukouyama et al., 2002). At E15.5, EPHB4$^+$ coronary veins were present in the subepicardial layer of the dorsal ventricular wall (Fig. 2A-D), whereas ephrin B2$^+$ coronary arteries were found in the myocardial layer (Fig. 2E-H). This distribution is consistent with that reported in previous studies (Lavine et al., 2008; Red-Horse et al., 2010). Cardiac axons were detected in close proximity to large diameter vessels in the subepicardium but not in the myocardium, indicating that cardiac axons associate only with EPHB4$^+$ large diameter coronary veins at this stage (Fig. 2A,C,I).

In order to characterize the neuronal subtypes present at E15.5, we used calcitonin gene related peptide (CGRP; CALCA – Mouse Genome Informatics) as a marker for sensory neurons, tyrosine hydroxylase (TH) as a marker for sympathetic neurons, and choline acetyltransferase (ChAT) as a marker for parasympathetic neurons. Immunohistochemical staining for these markers revealed that the majority of axons in the dorsal ventricular subepicardium are TH$^+$ (Fig. 2J-M). A smaller number of ventricular axons were ChAT$^+$ (supplementary material Fig. S1), and no CGRP$^+$ axons were detected. Consistent with these results, other studies have found that CGRP$^+$ sensory innervation is barely detectable at E15.5 but appears by E18.5 (Ieda et al., 2006). These data indicate that autonomic innervation precedes sensory innervation in the developing heart, and that the initial neurovascular interactions during cardiac development are restricted to coronary veins and sympathetic nerves.

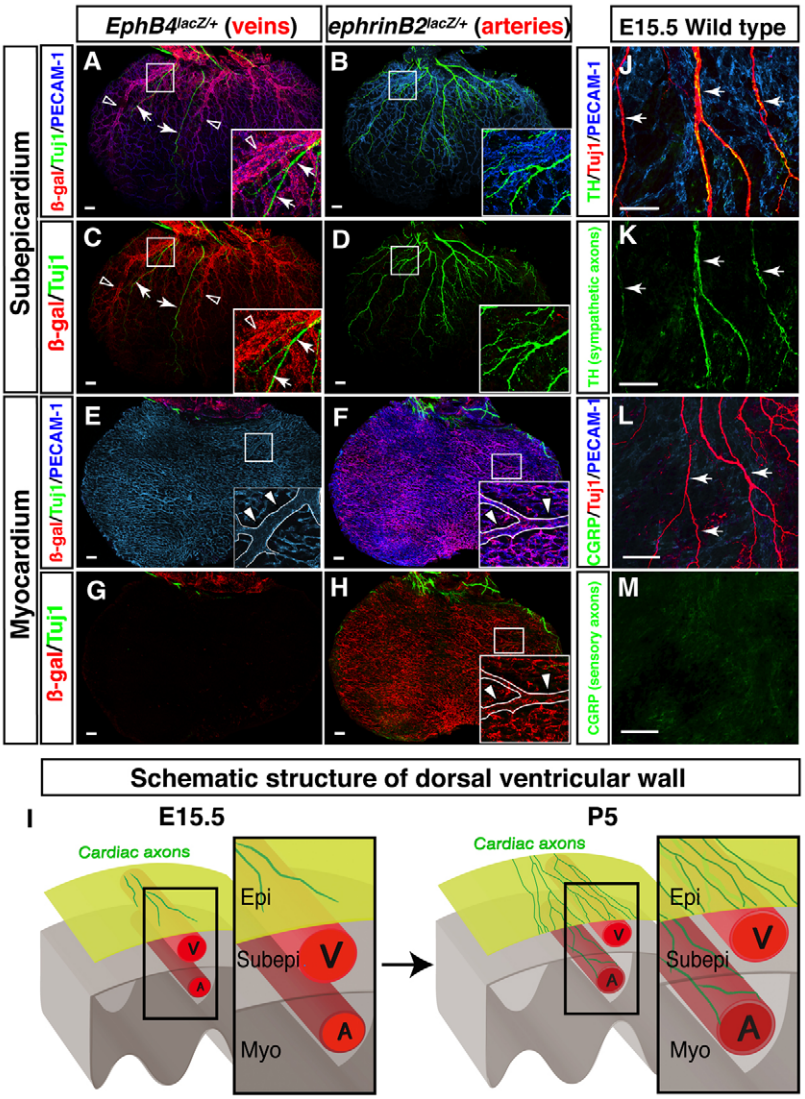

Fig. 2. Cardiac sympathetic axons associate with large diameter coronary veins within the subepicardial layer of the dorsal ventricular wall.
(**A-H**) The dorsal ventricular walls of E15.5 *EphB4*$^{taulacZ/+}$ (A,C,E,G; the venous marker EPHB4) or *ephrinB2*$^{taulacZ/+}$ (B,D,F,H; the arterial marker ephrin B2) hearts are shown. Whole-mount triple immunofluorescence confocal microscopy was performed with antibodies to PECAM1 (A,B,E,F, blue), TUJ1 (A-H, green) and β-galactosidase (A-H, red). Boxed regions in A-F,H are magnified in insets. (A-D) The subepicardium. Coronary veins expressing EphB4^{taulacZ} are clearly visible in *EphB4*$^{taulacZ/+}$ embryos (A,C). However, arteries expressing ephrinB2^{taulacZ} are barely detectable in *ephrinB2*$^{taulacZ/+}$ embryos (B,D). TUJ1^{+} cardiac axons (A,C, arrows) associate with EPHB4^{+} large diameter veins (A,C, open arrowheads). (E-H) The myocardium. Coronary arteries expressing ephrinB2^{taulacZ} cover the deeper layer in *ephrinB2*$^{taulacZ/+}$ embryos (F,H). One large diameter artery runs from the base towards the apex of the ventricle (E,F,H, insets, arrowheads). EphB4^{taulacZ}-expressing veins are barely detectable in *EphB4*$^{taulacZ/+}$ embryos (E,G). TUJ1^{+} cardiac axons are also not detected in the myocardial layer (E-H). (**I**) Schematic illustrating sympathetic innervation of the developing heart. By E15.5, coronary veins develop to form large diameter branches within the subepicardial layer (Subepi), where cardiac axons initiate distal axon extension. Coronary arteries develop separately, in the myocardial layer (Myo). By P5, cardiac axons extend into the myocardial layer (see supplementary material Fig. S2). These axons innervate large diameter coronary arteries as final targets. Epi, epicardial layer; V, vein; A, artery. (**J-M**) Neuronal subtype characterization. E15.5 hearts were labeled with antibodies to the sympathetic neuron marker tyrosine hydroxylase (TH; J,K, green) or the sensory neuron marker calcitonin gene related peptide (CGRP; L,M, green) in addition to PECAM1 (J,L, blue) and TUJ1 (J,L, red). TUJ1^{+} nerves are mostly TH^{+}, indicating that these axons in the subepicardium are mostly sympathetic nerves (J,K, arrows). CGRP^{+} sensory innervation is not detectable at E15.5 (L,M, arrows). Scale bars: 100 μm.

Coronary remodeling is required for normal sympathetic innervation

To investigate the mechanism of the interaction between large diameter coronary veins and sympathetic nerves, we examined the temporal pattern of development for both networks. At E13.5, a primary capillary plexus covered the entire dorsal surface of the heart. Remodeled vessels and sympathetic axons were present only in a small area adjacent to the sinus venosus on the dorsal ventricular surface (supplementary material Fig. S2A). By contrast, the ventral surface exhibited an expanding vascular plexus and no detectable innervation (supplementary material Fig. S2D). By E14.5, vascular remodeling progressed dramatically (supplementary material Fig. S2B); all three large diameter branches were discernable and extended across the full subepicardial layer of the dorsal ventricular wall. Sympathetic axon extension, however, continued along large diameter vessels through E14.5 and did not reach the distal regions of the dorsal surface until E15.5 (supplementary material Fig. S2B,C). By this stage, the ventral surface began to display some remodeled vessels but sympathetic axons were still mostly absent (supplementary material Fig. S1E,F). After E15.5, sympathetic axons continued to associate with large diameter vessels in the dorsal surface (supplementary material Fig. S2G,H), and the ventral surface exhibited a similar pattern of vascular remodeling followed by innervation (supplementary material Fig. S2I,J). Importantly, vascular remodeling preceded sympathetic innervation throughout the subepicardium.

By postnatal day (P) 5, sympathetic axons extended into the myocardial layer of the dorsal ventricular wall. These axons innervated large diameter coronary arteries (supplementary material Fig. S2L; Fig. 2I). Notably, in the subepicardial layer, no obvious sympathetic innervation of veins was detectable despite congruent branching of sympathetic nerves and large coronary veins (supplementary material Fig. S2K). These findings suggest that sympathetic axons extend within the subepicardium using large diameter coronary veins only as an intermediate template en route to their final targets in the myocardium, such as coronary arteries.

Because vascular remodeling precedes axon extension, we examined whether the pattern of vascular remodeling affects that of innervation. The stereotypical pattern of the coronary vasculature is disrupted in conditional β-catenin (*Ctnnb1*) mutant mice that lack β-catenin expression in the epicardium (Zamora et al., 2007). Systemic ablation of the β-catenin transcription factor causes lethality early in embryonic development, but conditional deletion using *Gata5-Cre* allows survival until at least E18.5 (Zamora et al., 2007). In *Gata5-*

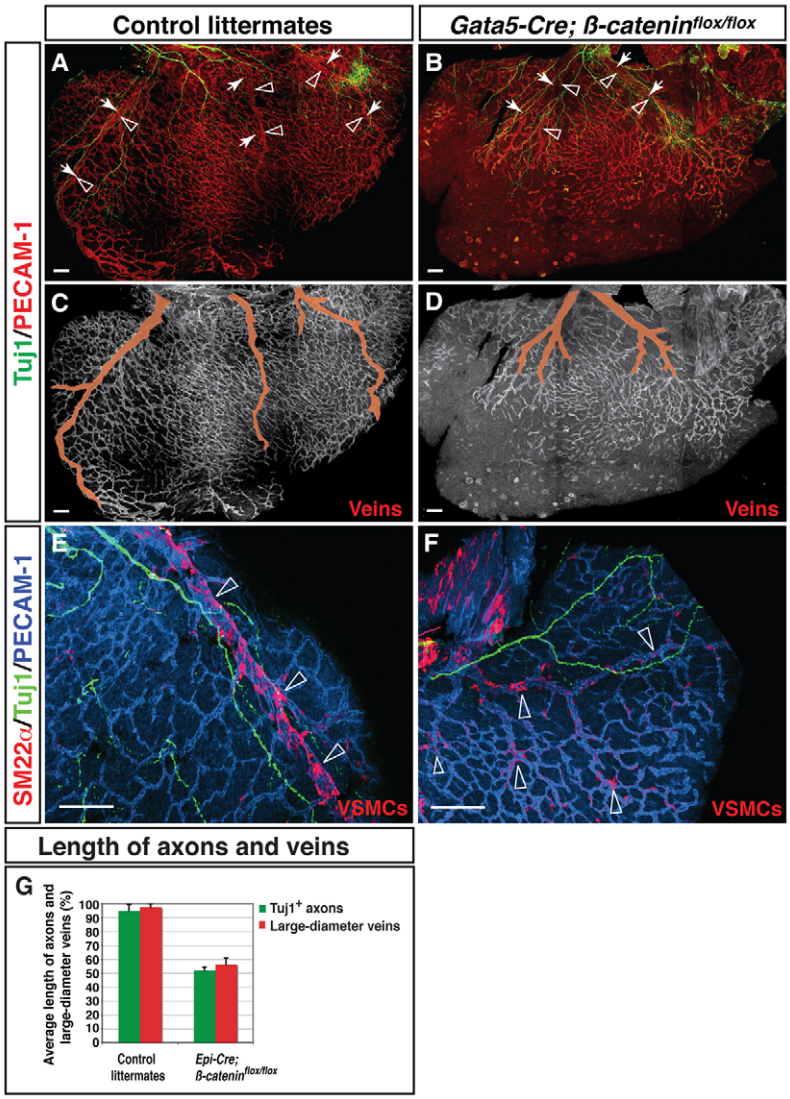

Fig. 3. Defective coronary development leads to abnormal sympathetic innervation. (**A-D**) Dorsal ventricular walls of *Gata5-Cre; β-catenin*$^{flox/flox}$ mutants (B,D) and control littermates (A,C) at E15.5. Double immunofluorescence confocal microscopy was performed with antibodies to PECAM1 (A,B, red; C,D, white) and TUJ1 (A-D, green). In *Gata5-Cre; β-catenin*$^{flox/flox}$ mice the pattern of coronary remodeling appears disorganized compared with control littermates (A versus B, open arrowheads; C versus D, pseudocolored in red). The mutants also exhibit abnormal sympathetic innervation (A versus B, arrows). Both large diameter veins and sympathetic axons fail to fully develop in the subepicardium. (**E**,**F**) Vascular smooth muscle cell (VSMC) recruitment. Triple staining with antibodies to the VSMC marker SM22α (E,F, red) in addition to PECAM1 (E,F, blue) and TUJ1 (E,F, green) revealed that SM22α^{+} VSMCs associate less strongly with large diameter veins in these mutants; SM22α^{+} VSMCs are distributed more uniformly throughout the subepicardium, indicating defects in angiogenic remodeling (E versus F, open arrowheads, G). (**G**) Quantification of nerve-vessel association. The length of large diameter vessels and of sympathetic axons is significantly affected in *Gata5-Cre; β-catenin*$^{flox/flox}$ mutants. Length is measured as a percentage of distance from base to apex. Control littermates, *n*=3; *Gata5-Cre; β-catenin*$^{flox/flox}$ mutants, *n*=3; error bars indicate s.e.m. Scale bars: 100 μm.

Cre; β-catenin$^{flox/flox}$ mice, the coronary vasculature is disorganized relative to the stereotypical pattern found in control littermates (Fig. 3A-D). In addition, SM22α^{+} VSMCs associated less strongly with large diameter veins in these mutants and were distributed more uniformly throughout the subepicardium (Fig. 3E,F). The unusual pattern of VSMCs indicates that critical steps of angiogenic remodeling have been disrupted. Notably, these coronary defects were accompanied by abnormal sympathetic innervation (Fig. 3G). In the mutants, sympathetic axons failed to fully innervate the subepicardial layer of the dorsal ventricular wall (Fig. 3A,B). Some sympathetic axons still appeared to associate with abnormally branched large diameter coronary veins, albeit to a lesser extent than in the control (Fig. 3B). By contrast, examination of *Phox2b*$^{-/-}$ mutants with defective cardiac innervation showed no vascular abnormalities (supplementary material Fig. S3). These results suggest that proper coronary remodeling is required for the observed neurovascular association, whereas cardiac axon growth does not affect the pattern of vascular remodeling.

VSMC distribution closely mirrors sympathetic axon distribution

The recruitment of VSMCs to large diameter vessels is a significant step during angiogenic remodeling. In addition, previous studies have demonstrated that VSMCs are a likely source of growth factors that can act on sympathetic axons (reviewed by Glebova and Ginty, 2005). Indeed, SM22α^{+} VSMCs were found predominantly in nerve-associated large diameter veins at E15.5 (Fig. 4A-C′). This distribution was confirmed with immunohistochemical staining of *SM22α-lacZ* embryonic hearts, which have a *lacZ* reporter to detect expression of *SM22α* (*Tagln* – Mouse Genome Informatics) (data not shown). It is also important to note that the distribution of SM22α^{+} VSMCs is strikingly similar to that of axons. As with axons, the majority of VSMCs are found around remodeled vessels, but a small number can be found in regions between these branches (Fig. 4D,D′). These data suggest that subepicardial SM22α^{+} VSMCs might be involved in signaling between veins and sympathetic axons.

Coronary VSMCs secrete a diffusible signal that influences the pattern of sympathetic axon growth *in vitro*

Impairment of sympathetic innervation in *Gata5-Cre; β-catenin*$^{flox/flox}$ mutants provides strong evidence that vascular remodeling influences axon extension. However, abnormal signals from VSMCs in disrupted coronary veins might not be solely responsible for defects in innervation in these mutants. Atypical

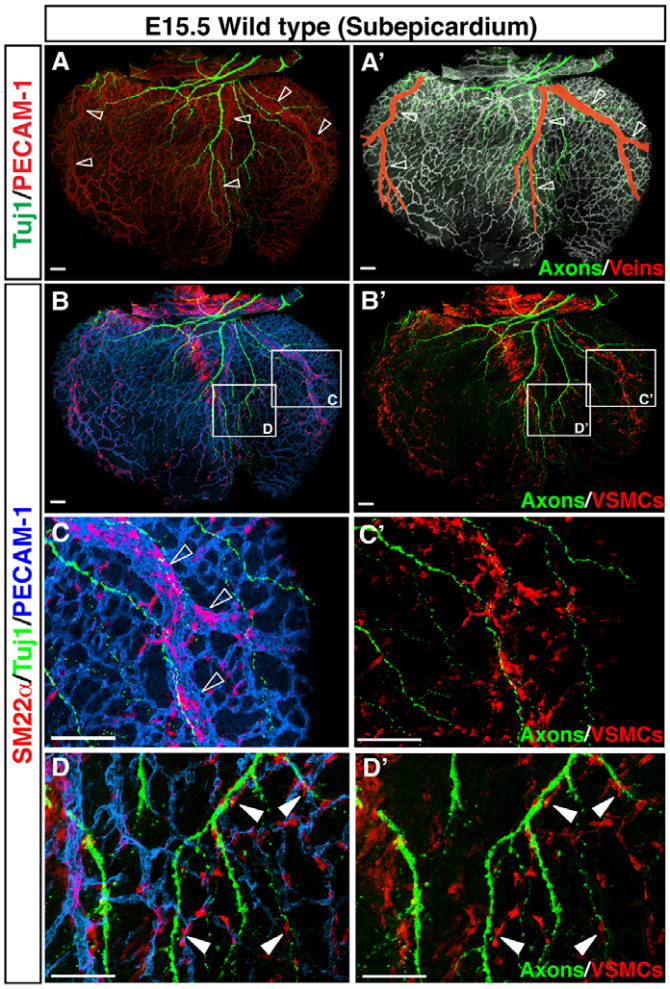

Fig. 4. VSMCs cover nerve-associated large diameter coronary veins. (**A-D′**) Visualization of coronary VSMCs in the subepicardium. Whole-mount triple immunofluorescence confocal microscopy was performed with antibodies to the VSMC marker SM22α (B-D′, red) in addition to PECAM1 (A, red; A′, white; B-D, blue) and TUJ1 (green). Magnified images (C-D′) show the boxed regions in B,B′. At E15.5, SM22α^{+} VSMCs are found predominantly around nerve-associated large diameter coronary veins (A-C′, open arrowheads), and a smaller number of SM22α^{+} VSMCs are located between remodeled veins (D,D′, arrowheads). Scale bars: 100 μm.

sympathetic innervation might instead be secondary to signal defects caused by leaky activity of *Gata5-Cre* expression in the myocardium. Therefore, we turned to *in vitro* culture experiments to directly examine whether coronary VSMCs guide sympathetic axon outgrowth.

We initially isolated coronary VSMCs and sympathetic ganglia (SG) from embryos at E13.5, the stage at which sympathetic axons begin to innervate the subepicardial layer (supplementary material Fig. S2A). Since coronary VSMCs originate from epicardial cells (Mikawa and Fischman, 1992; Cai et al., 2008; Zhou et al., 2008), we dissected cardiac ventricles from E12.5 or E13.5 embryos and cultured them to isolate migrating epicardial cells on a collagen gel (Fig. 5A). VSMCs were obtained from the differentiation of isolated epicardial cells and VSMC aggregates were generated in hanging drop culture (Fig. 5A). We confirmed the identity of the cultured cells by immunostaining for VSMC markers such as SM22α, αSMA and SM-MHC (Fig. 5B,C). SG explants cultured alone demonstrated minimal axon outgrowth (supplementary material Fig. S4A-D). By contrast, SG explants cultured with VSMC aggregates showed robust axon outgrowth (Fig. 5D). Axons projected extensively and preferentially towards VSMC aggregates (Fig. 5D-H, compare 5E with 5F). These results demonstrate that coronary VSMCs secrete a diffusible factor that promotes sympathetic axon outgrowth.

Additionally, we examined whether myocardial tissue was also able to induce directional sympathetic axon outgrowth. Explants of E13.5 myocardial tissue failed to stimulate axon outgrowth from both E13.5 and E16.5 SG explants (Fig. 5I,J,M,N). By contrast, E16.5 myocardial tissue explants successfully induced directional axon outgrowth from both E13.5 and E16.5 SG explants (Fig. 5K-N). These results are consistent with our timecourse analysis, which shows that sympathetic innervation of the myocardium begins after E15.5 (supplementary material Fig. S2A). Furthermore, primary epicardial tissue explants did not promote directional axon extension from SG explants (supplementary material Fig. S4E). These experiments demonstrate that coronary VSMCs, but not early myocardial or epicardial tissues, secrete a neurotrophic signal that mediates sympathetic axon extension in the subepicardium. Subsequently, cells in myocardial tissue provide a signal that directs sympathetic axons into the deeper myocardial layer.

Coronary venous VSMC-derived NGF mediates sympathetic axon extension

We next used our SG and VSMC co-culture system to identify a coronary VSMC-derived signal that is responsible for sympathetic axon growth. First, we surveyed differential expression of candidate neurotrophic factors and receptors (84 genes in total) from coronary VSMCs relative to myocardial tissues from E13.5 hearts using an RT-PCR array method. We found that artemin (*Artn*), endothelin 1 (*Edn1*), glia maturation factors β and γ (*Gmfb* and *Gmfg*), neuregulin 1 (*Nrg1*) and nerve growth factor (*Ngf*) were more highly expressed in VSMCs than in myocardial tissues (data not shown). Further, a semi-quantitative RT-PCR analysis confirmed the differential expression of *Artn*, *Gmfb*, *Gmfg*, *Nrg1* and *Ngf* between VSMCs and myocardial tissues (Fig. 6A). Of these six candidate factors, NGF expression was clearly detected in coronary VSMCs in the subepicardium by immunohistochemical staining (Fig. 6B,D,E) and *in situ* hybridization (Fig. 6C). These observations were supported by the analysis of an *NGF$^{lacZ/+}$* reporter strain to identify NGF-expressing cells (Fig. 6F). Expression of ARTN and NRG1 was also detected in coronary VSMCs (supplementary material Fig. S5A-D,Q-T; data not shown). The remaining candidates were not detected by immunohistochemical staining or *in situ* hybridization analysis (supplementary material Fig. S5E-P; data not shown).

We next examined which factors can promote axon outgrowth from SG explants *in vitro*. E13.5 SG explants were responsive to ARTN, EDN1, NRG1 and NGF, but displayed little or no axon outgrowth when exposed to GMFβ or GMFγ (supplementary material Table S2). To inhibit the action of these four candidates on SG explants, we employed EDN1 receptor-selective antagonists (BQ123 for endothelin receptor type A; BQ788 for endothelin receptor type B) and neutralizing antibodies against ARTN, NRG1 or NGF. Each inhibitor successfully blocked the effect of its factor on SG explants (supplementary material Fig. S6).

We next tested whether these inhibitors could block VSMC-mediated axon outgrowth from SG explants *in vitro*. Among them, only the NGF-neutralizing antibody (anti-NGF NZAb) could selectively inhibit directional axon outgrowth as compared with a control isotype IgG (Fig. 6G-I). When the co-culture system was

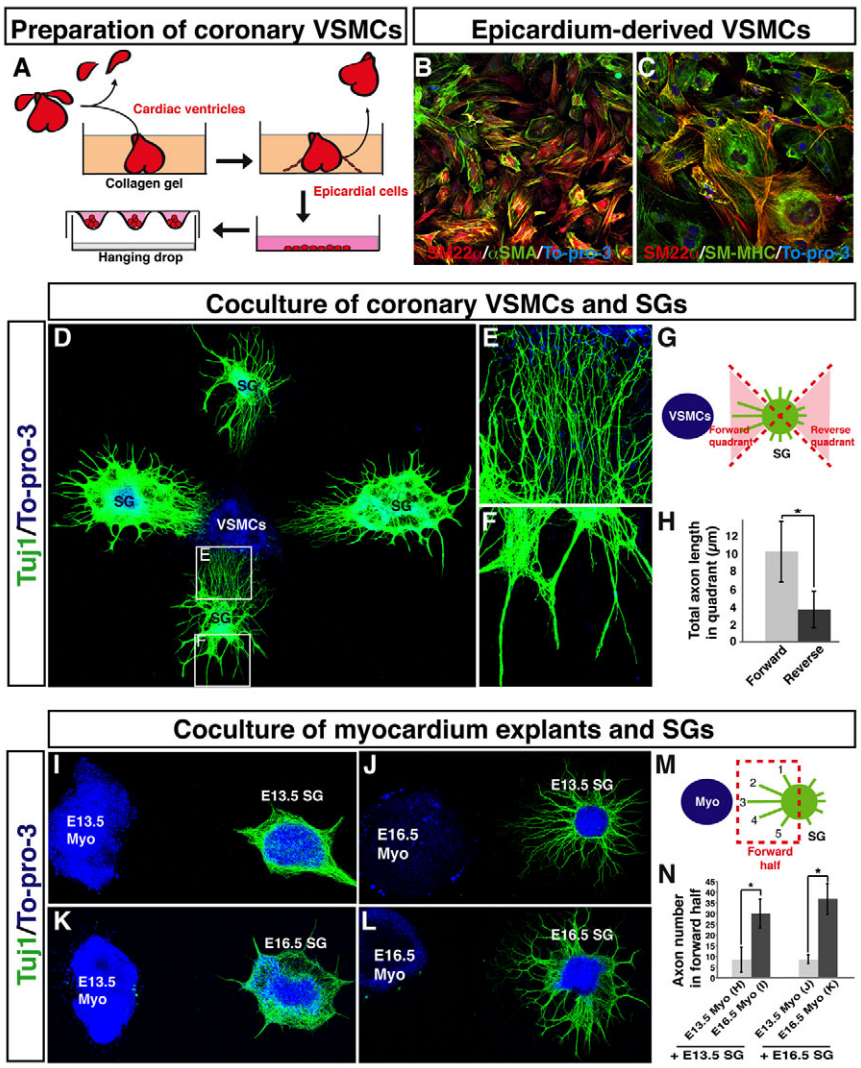

Fig. 5. Fetal epicardium-derived VSMCs promote axon outgrowth from fetal sympathetic ganglia *in vitro*. (**A**) Schematic illustrating the preparation of coronary VSMCs. E12.5 or E13.5 cardiac ventricles were cultured in collagen gel for 2 days. The ventricles were removed from the gel, and migrated epicardial cells were harvested and further expanded on a type IV collagen-coated dish. VSMC aggregations were obtained using a hanging drop culture method. (**B**,**C**) Primary culture of epicardial-derived VSMCs stained with antibodies to VSMC markers SM22α (B,C, green) and αSMA (B, red), and SM-MHC (C, green), together with the nuclear dye To-pro-3 (blue). (**D-H**) Co-culture of coronary VSMCs and sympathetic ganglia (SG). E13.5 fetal SG were cultured with VSMC aggregations obtained as in A and stained with anti-TUJ1 antibody (green) and To-pro-3 (blue). Magnified images (E,F) show the boxed regions in D. Note that directional axon outgrowth towards VSMCs was observed (E). The total lengths of axons in the forward and reverse quadrants (G) were calculated using Volocity (H). n=19. (**I-N**) Co-culture of myocardium explants and SG. SG were cultured with fetal myocardial tissue explants and labeled with anti-TUJ1 antibody (green) and To-pro-3 (blue). E13.5 myocardial tissue explants failed to stimulate axon outgrowth from E13.5 and E16.5 SG explants (I,K), whereas E16.5 myocardial tissue explants successfully induced directional axon outgrowth from both E13.5 and E16.5 SG explants (J,L). The total number of axons in the forward region (M) for each sample was quantified using Volocity (N). E13.5 SG with E13.5 myo, n=7; E13.5 SG with E16.5 myo, n=8; E16.5 SG with E13.5 myo, n=5, E16.5 SG with E16.5 myo, n=6. *P<0.01 (Student's t-test); error bars indicate s.e.m. Myo, myocardium.

treated with this antibody, we observed random and non-directional axon outgrowth, and axons appeared more fasciculated (Fig. 6H). Further, the level of inhibition varied with the concentration of the antibody (Fig. 6I). The other inhibitors, alone or in combination, showed no effect at any tested concentrations (supplementary material Fig. S6D-Z).

To further confirm that directional axon outgrowth depended on VSMC-derived NGF, we employed a knockdown of *Ngf* in VSMCs using a lentiviral vector carrying *Ngf* shRNA during primary culture. Compared with control shRNA-infected VSMCs, the *Ngf* knockdown reduced NGF expression by more than 50% (Fig. 6J). These *Ngf*-deficient VSMCs failed to induce preferential directional axon outgrowth from the SG explants (Fig. 6K-M). These data suggest that VSMCs secrete NGF to promote directional axon outgrowth from sympathetic nerves. Indeed, NGF-soaked beads successfully promoted directional axon outgrowth from SG explants (supplementary material Fig. S7A-B′), demonstrating that NGF is both necessary and sufficient for VSMC-mediated guidance *in vitro*.

NGF is required for cardiac sympathetic innervation *in vivo*

An *in vivo* demonstration in support of these *in vitro* results would require a coronary VSMC-specific knockout of *Ngf*, but the floxed *Ngf* allele is not currently available. A definitive test of whether NGF serves as a chemotactic factor for directional axon growth *in vivo* was accomplished by implantation of beads coated with anti-NGF NZAb on the dorsal surface of chick heart. In E10 hearts implanted with control isotype IgG beads, TUJ1$^+$ axons fully extended along with αSMA$^+$ VSMC-covered large diameter vessels (Fig. 6N). In hearts with anti-NGF NZAb beads, the axons failed to extend into the regions where the beads were placed (Fig. 6O), despite the normal formation of large vessels (Fig. 6N). Quantification indicated an ~50% reduction in axon extension along the large vessels in the hearts implanted with neutralizing antibody (Fig. 6P).

We next examined whether the ectopic presence of NGF causes precocious innervation on the dorsal surface of chick heart. At E10, the distal portion of αSMA$^+$ VSMC-covered large diameter vessels did not accompany TUJ1$^+$ axons in the control (data not shown) or in the presence of BSA-soaked beads (supplementary material Fig. S7C). By contrast, NGF-soaked beads successfully recruited TUJ1$^+$ axons (supplementary material Fig. S7D). Cumulatively, these results suggest that local NGF secretion from coronary VSMCs in the subepicardium is required for sympathetic axon growth along large diameter coronary vessels in the developing heart.

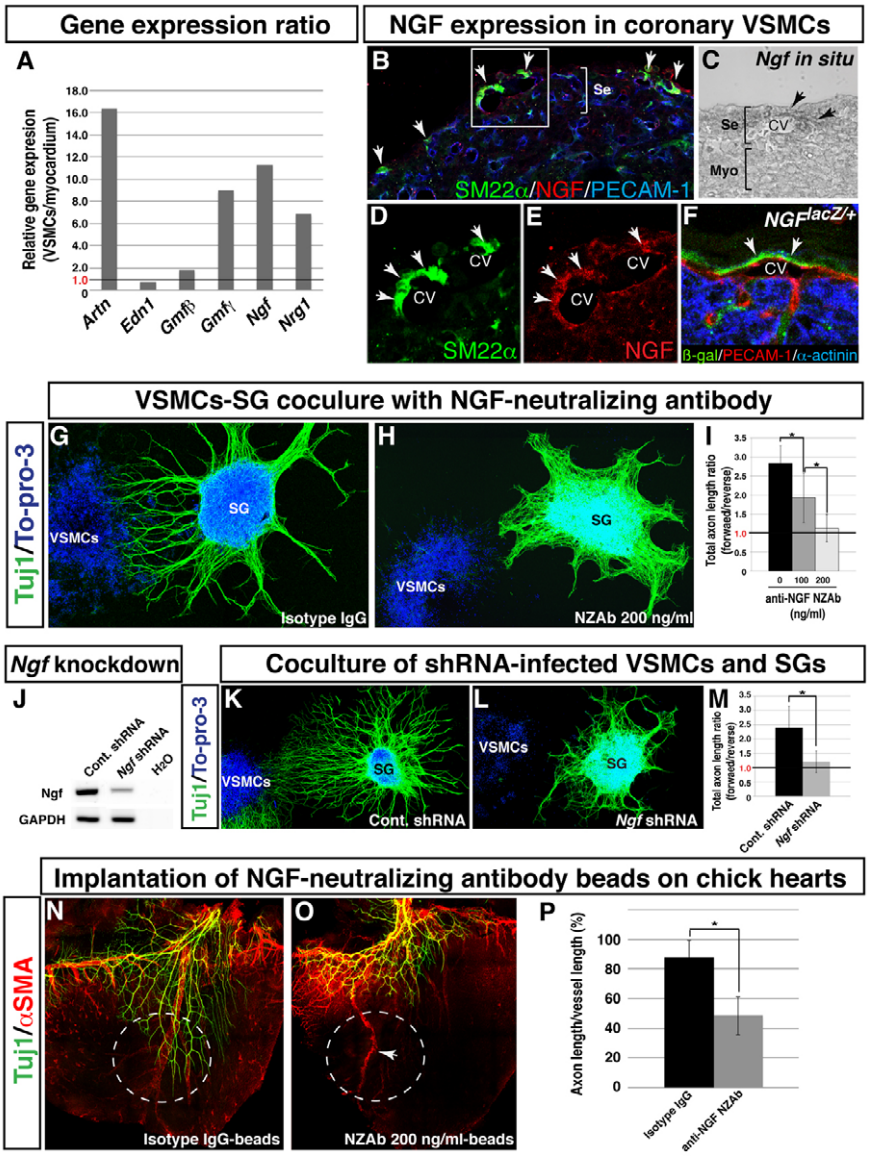

Fig. 6. Coronary VSMCs stimulate directional axon growth by NGF *in vitro*. (**A**) Semi-quantitative RT-PCR analysis showing differential expression of neurotrophic factors as indicated between VSMCs and E13.5 myocardial tissues. A ratio exceeding 1.0 indicates that the factor is more highly expressed in VSMCs than in myocardial tissues. (**B-F**) NGF expression in coronary VSMCs in the subepicardium. Triple immunofluorescence confocal microscopy of E15.5 heart sections was performed using antibodies to SM22α (B,D, green) and NGF (B,E, red) as well as PECAM1 (B, blue). Magnified images (D,E) show the boxed region in B. NGF expression was detected in venous VSMCs in the subepicardium (B,D,E, arrows). *In situ* hybridization with *Ngf* RNA probes on E15.5 heart section shows that *Ngf* mRNA is expressed in coronary veins in the subepicardium (C, arrows). The NGF-expressing cells were also detected in coronary veins by triple staining of E15.5 $NGF^{lacZ/+}$ reporter heart sections with antibodies for β-gal (green), PECAM1 (red) and the myocardial cell marker α-actinin (blue) (F, arrows). CV, coronary vein; Se, subepicardium; Myo, myocardium. (**G-I**) VSMC-mediated directional axon outgrowth is attenuated by anti-NGF neutralizing antibody (NZAb). E13.5 SG were cultured with VSMC aggregations in the presence of control isotype IgG (G) or 200 ng/ml anti-NGF NZAb (H), and were labeled with anti-TUJ1 antibody (green) and To-pro-3 (blue). Anti-NGF NZAb selectively inhibited directional axon outgrowth as compared with control isotype IgG. The level of inhibition varies with the concentration of anti-NGF NZAb (I). The total lengths of axons in the forward and reverse quadrants (see Fig. 5M) were calculated using Volocity. The ratios of the total lengths of axons in the forward versus reverse quadrants are shown (I). A ratio above 1.0 indicates directional axon outgrowth towards VSMC aggregates. **P*<0.05 (Student's *t*-test); isotype IgG, *n*=8; 100 ng/ml anti-NGF NZAb, *n*=5; 200 ng/ml anti-NGF NZAb, *n*=6. (**J-M**) *Ngf*-deficient VSMCs fail to induce directional axon outgrowth. VSMCs were infected with a control or *Ngf* shRNA lentivirus during primary epicardial culture. The expression levels of *Ngf* were assessed by RT-PCR analysis (J). E13.5 SG were cultured with control VSMCs (K) or *Ngf*-deficient VSMCs (L) and labeled with anti-TUJ1 antibody (green) and To-pro-3 (blue). *Ngf*-deficient VSMCs failed to induce preferential directional axon outgrowth. Directional outgrowth was quantified as in Fig. 5G (M). **P*<0.05 (Student's *t*-test); control shRNA-infected VSMCs, *n*=3; *Ngf* shRNA-infected VSMCs, *n*=5. (**N-P**) Effect of anti-NGF NZAb on coronary VSMC-mediated sympathetic axon growth in chick embryonic hearts. Control isotype IgG-soaked beads or anti-NGF NZAb-soaked beads were implanted on the dorsal surface of E6 chick hearts. After 4 days of incubation, the hearts were dissected for whole-mount double immunofluorescence confocal microscopy using antibodies to TUJ1 (N,O, green) and αSMA (N,O, red). Control beads have no effect (N, white dashed circle) and anti-NGF NZAb beads show no distal extension of sympathetic axons (O, white dashed circle). Distal axon extension was quantified (P). **P*<0.01 (Student's *t*-test); isotype IgG, *n*=5; anti-NGF NZAb, *n*=5. Note that anti-NGF NZAb beads do not inhibit the formation of large diameter coronary vessels (O, arrow). Error bars indicate s.e.m.

Arterial VSMC-derived NGF is responsible for subsequent axon penetration into the myocardium at a late stage of cardiac development

We next sought to determine what controls axon penetration into the myocardium after distal extension in the subepicardium. Unlike at E13.5, E16.5 myocardial explants secrete chemoattractants to stimulate sympathetic axon growth. Indeed, average NGF expression is highly enhanced in E16.5 myocardial tissue compared with E13.5 myocardium (Fig. 7A). To more precisely localize NGF-expressing cells in the myocardium, we utilized an *NGF*$^{lacZ/+}$ reporter strain that allows us to detect NGF expression with greater spatial resolution than previously possible. Consistent with the analysis by whole-mount staining (Fig. 2), section staining of *EphB4*$^{taulacZ/+}$ and *ephrinB2*$^{taulacZ/+}$ cardiac ventricles revealed that EPHB4^{+} coronary veins and ephrin B2^{+} arteries were present in the subepicardium and myocardium, respectively (Fig. 7B-D). Surprisingly, NGF expression appeared to be restricted to VSMCs throughout the heart (Fig. 7E-L). Based on the distinct localization of cardiac arteries and veins, myocardial NGF expression is therefore limited to arterial VSMCs. At E15.5, NGF expression in venous VSMCs proceeds distally in parallel with angiogenic remodeling and immediately preceding axon extension within the subepicardium (Fig. 7E,G,H). NGF expression was downregulated in venous VSMCs but not in arterial VSMCs near the sinus venosus, where axons had already completed their extension along the veins (Fig. 7E,F,H). By E17.5, no venous VSMCs expressed NGF at detectable levels, but arterial VSMCs in the myocardium demonstrated persistent NGF expression as axons extended into that layer (Fig. 7I-L). This dynamic pattern of NGF expression in cardiac VSMCs suggests that NGF might have a functional role as a chemoattractant.

We next examined whether VSMC-derived NGF mediates the chemotactic effect of the E16.5 myocardium explants on sympathetic axons. Anti-NGF NZAb clearly blocked E16.5 myocardium-mediated directional axon outgrowth *in vitro* (Fig. 7M-O). These data suggest that arterial VSMCs secrete NGF to stimulate sympathetic axon growth into the myocardial layer. Furthermore, this sequential expression pattern of NGF in venous VSMCs in the subepicardium and arterial VSMCs in the myocardium is responsible for a coordinated process of distal axon extension in the developing heart (Fig. 8).

DISCUSSION

In this study, we show that cardiac sympathetic axons are preferentially aligned with large diameter coronary veins in the

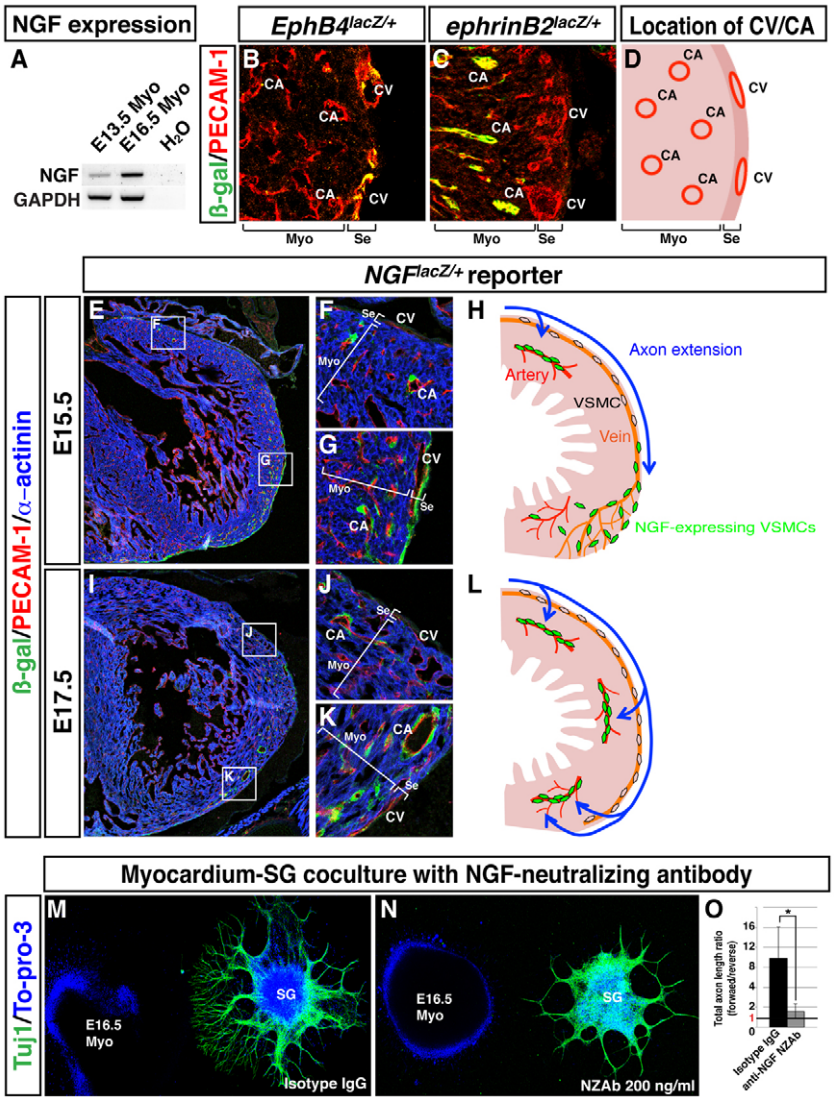

Fig. 7. Dynamic expression of NGF in VSMCs from the subepicardium to the myocardium is responsible for myocardial innervation. (**A**) RT-PCR analysis of E13.5 and E16.5 myocardium explants. (**B-D**) Location of EPHB4^{+} coronary veins (B) and ephrin B2^{+} arteries (C) in the cardiac ventricles. Sections of *EphB4*$^{lacZ/+}$ (B) and *ephrinB2*$^{lacZ/+}$ (C) hearts were stained with antibodies for β-gal (green) and PECAM1 (red). The relative location of coronary veins (CV) and arteries (CA) in heart ventricle is shown in D. (**E-L**) NGF expression analysis on *NGF*$^{lacZ/+}$ reporter heart sections. E15.5 (E-G) or E17.5 (I-K) heart sections of *NGF*$^{lacZ/+}$ reporter embryos were stained with antibodies for β-gal (green), PECAM1 (red) and α-actinin (blue). Magnified images (F,G,J,K) show the boxed regions in E,I. Schematic models illustrating dynamic expression of NGF in VSMCs in parallel with sympathetic axon extension at E15.5 (H) and E17.5 (L). (**M-O**) SG and myocardium co-culture with anti-NGF NZAb. E16.5 SG were cultured with E16.5 myocardial explants in the presence of 200 ng/ml isotype IgG (M) or 200 ng/ml anti-NGF NZAb (N). The culture was stained with anti-TUJ1 antibody (green) and To-pro-3 (blue). (O) Directional axon growth was quantified as in Fig. 5G. *P<0.02 (Student's t-test); isotype IgG, n=5; 200 ng/ml anti-NGF NZAb, n=5; error bars indicate s.e.m. CV, coronary vein; CA, coronary artery; Myo, myocardium; Se, subepicardium.

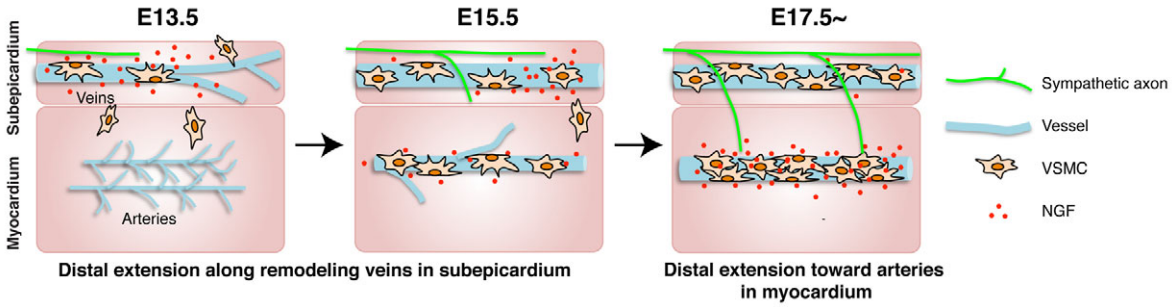

Fig. 8. A two-step process is responsible for sympathetic innervation of the developing heart. Model for sympathetic axon innervation of the developing mouse heart. At E13.5, coronary veins undergo angiogenic remodeling in the subepicardium. Venous VSMCs transiently secrete NGF as they associate with remodeled veins. Sympathetic axons start to extend into the subepicardium. By E15.5, NGF expression in venous VSMCs proceeds distally in parallel with vascular remodeling, and axons extend along newly formed veins. Some arterial VSMCs begin to express NGF in the myocardium. By E17.5, which is the stage when sympathetic innervation penetrates the myocardium, NGF expression is detected only in arterial VSMCs.

subepicardial layer of the dorsal ventricular wall in the developing heart. Our results suggest that sympathetic innervation of myocardial arteries proceeds by a two-step process (Fig. 8). First, coronary venous VSMC-derived NGF mediates sympathetic axon extension along large diameter coronary veins within the subepicardium. After axons complete their extension within that layer, they penetrate into the myocardial layer guided by arterial VSMC-derived NGF.

Cardiac sympathetic axons associate with large diameter coronary veins

Our whole-mount immunohistochemical analysis of the developing heart has revealed a novel neurovascular association. In the subepicardium, sympathetic axons branch alongside large diameter veins. By contrast, earlier studies have demonstrated that arteries align with sensory nerves in the developing limb skin (Mukouyama et al., 2002) and that sympathetic axons extend from SG along arteries (Luff, 1996; Glebova and Ginty, 2005). To our knowledge, no studies have yet reported an interaction between sympathetic nerves and veins. Our observations reflect the characteristic distribution of coronary veins and arteries in the ventricular wall of the developing heart.

Large diameter coronary veins serve as intermediate conduits for distal sympathetic axon extension via VSMC-derived NGF

Our findings suggest that coronary VSMCs induce sympathetic axon extension via local secretion of NGF. This is surprising because NGF has primarily been implicated in the innervation of final target cells, rather than distal axon extension (Levi-Montalcini, 1987). The dynamic pattern of NGF expression in coronary VSMCs provides strong evidence that NGF directs sympathetic axon growth, as previous work has demonstrated similar patterns in other chemoattractants. For example, ARTN expression in VSMCs shifts from central to peripheral blood vessels in parallel with sympathetic axon extension along these vessels (Honma et al., 2002). In the developing heart, NGF is important for sympathetic innervation of the myocardium (Hassankhani et al., 1995; Ieda et al., 2004). In *Ngf*$^{-/-}$; *Bax*$^{-/-}$ embryos, there appears to be normal sympathetic axon extension along the extracardiac vasculature but a drastic decrease in sympathetic innervation of the heart (Glebova and Ginty, 2004). These studies suggest that NGF is required for the sympathetic innervation of target organs but not for proximal axon extension along blood vessels. However, these studies did not address the role that NGF plays in determining the pattern of sympathetic innervation within the heart. We find that NGF is transiently expressed by VSMCs in coronary veins at the stage when sympathetic axons extend throughout the subepicardium (supplementary material Fig. S2I versus S2L). This brief period of expression might explain why axons follow veins during remodeling but fail to innervate them as final targets. Together, these results indicate that local secretion of NGF by VSMCs in coronary veins provides a template for sympathetic axon extension in the subepicardium.

Sympathetic innervation of the heart is a two-step process

Beginning at E13.5, angiogenic remodeling moves outward from the sinus venosus in the subepicardial layer. As VSMCs are recruited to newly formed veins, they transiently express NGF, stimulating axon extension along the vessels as they form. While subepicardial VSMCs downregulate NGF expression after venous remodeling, myocardial VSMCs begin to secrete NGF during arterial remodeling. These observations suggest that a two-step process is responsible for sympathetic innervation of the developing heart (Fig. 8). The mechanisms that control spatiotemporal changes in NGF expression by VSMCs merit further study, as precisely localized expression is crucial to cardiac innervation. Transient expression of NGF by venous VSMCs enables veins to function as a template but avoid innervation. Later, persistent NGF expression by arterial VSMCs allows for final target innervation in the myocardium.

The involvement of other signals in final target innervation of the myocardium remains under investigation. Previous work has provided a supportive mechanism in which SEMA3A, a myocardial cell-derived chemorepellent, may establish a restrictive environment that prevents sympathetic axon growth in the myocardium during subepicardial extension (Ieda et al., 2007). Whether cells other than VSMCs in the myocardium provide distinct innervation cues in a time-specific fashion remains to be addressed. Our results suggest that target organs of SG might possess stereotypical templates for distal extension and innervation that are adapted to their complex tissue structure and physiology.

Acknowledgements

We thank C. Lo and D. Alpert for breeding *SM22α*$^{lacZ/+}$ mice; J. F. Brunet and M. German for *Phox2b* mutant mice; M. Kotlikoff for *ChAT*^{BAC}*-eGFP* mice; D. Ginty for *NGF*$^{lacZ/+}$ mice; J. Hawkins and the staff of the NIH Bldg50 animal facility for assistance with mouse breeding and care; C. Combs and D. Malide for digital video editing; K. Gill for laboratory management and technical support; Y. Carter and R. Reed for administrative assistance; A. M. Michelson,

R. S. Balaban, R. S. Adelstein and X. Ma for invaluable help and discussion; M. Conti for editorial advice on the manuscript; and other members of the Laboratory of Stem Cell and Neuro-Vascular Biology for technical help and thoughtful discussion.

Funding
This work was supported by the Intramural Research Program of the National Heart, Lung and Blood Institute, National Institutes of Health (NIH) [HL006116 to Y.-s.M.] and was also supported by NIH grants [HL065484 and HL086879 to P.R.-L.]. Deposited in PMC for release after 12 months.

Competing interests statement
The authors declare no competing financial interests.

Supplementary material
Supplementary material available online at
http://dev.biologists.org/lookup/suppl/doi:10.1242/dev.087601/-/DC1

References

Cai, C. L., Martin, J. C., Sun, Y., Cui, L., Wang, L., Ouyang, K., Yang, L., Bu, L., Liang, X., Zhang, X. et al. (2008). A myocardial lineage derives from Tbx18 epicardial cells. *Nature* **454**, 104-108.
Carmeliet, P. and Tessier-Lavigne, M. (2005). Common mechanisms of nerve and blood vessel wiring. *Nature* **436**, 193-200.
Ciszek, B., Skubiszewska, D. and Ratajska, A. (2007). The anatomy of the cardiac veins in mice. *J. Anat.* **211**, 53-63.
Enomoto, H., Crawford, P. A., Gorodinsky, A., Heuckeroth, R. O., Johnson, E. M., Jr and Milbrandt, J. (2001). RET signaling is essential for migration, axonal growth and axon guidance of developing sympathetic neurons. *Development* **128**, 3963-3974.
Francis, N., Farinas, I., Brennan, C., Rivas-Plata, K., Backus, C., Reichardt, L. and Landis, S. (1999). NT-3, like NGF, is required for survival of sympathetic neurons, but not their precursors. *Dev. Biol.* **210**, 411-427.
Gerety, S. S., Wang, H. U., Chen, Z. F. and Anderson, D. J. (1999). Symmetrical mutant phenotypes of the receptor EphB4 and its specific transmembrane ligand ephrin-B2 in cardiovascular development. *Mol. Cell* **4**, 403-414.
Glebova, N. O. and Ginty, D. D. (2004). Heterogeneous requirement of NGF for sympathetic target innervation in vivo. *J. Neurosci.* **24**, 743-751.
Glebova, N. O. and Ginty, D. D. (2005). Growth and survival signals controlling sympathetic nervous system development. *Annu. Rev. Neurosci.* **28**, 191-222.
Hassankhani, A., Steinhelper, M. E., Soonpaa, M. H., Katz, E. B., Taylor, D. A., Andrade-Rozental, A., Factor, S. M., Steinberg, J. J., Field, L. J. and Federoff, H. J. (1995). Overexpression of NGF within the heart of transgenic mice causes hyperinnervation, cardiac enlargement, and hyperplasia of ectopic cells. *Dev. Biol.* **169**, 309-321.
Hildreth, V., Anderson, R. H. and Henderson, D. J. (2009). Autonomic innervation of the developing heart: origins and function. *Clin. Anat.* **22**, 36-46.
Honma, Y., Araki, T., Gianino, S., Bruce, A., Heuckeroth, R., Johnson, E. and Milbrandt, J. (2002). Artemin is a vascular-derived neurotropic factor for developing sympathetic neurons. *Neuron* **35**, 267-282.
Ieda, M., Fukuda, K., Hisaka, Y., Kimura, K., Kawaguchi, H., Fujita, J., Shimoda, K., Takeshita, E., Okano, H., Kurihara, Y. et al. (2004). Endothelin-1 regulates cardiac sympathetic innervation in the rodent heart by controlling nerve growth factor expression. *J. Clin. Invest.* **113**, 876-884.
Ieda, M., Kanazawa, H., Ieda, Y., Kimura, K., Matsumura, K., Tomita, Y., Yagi, T., Onizuka, T., Shimoji, K., Ogawa, S. et al. (2006). Nerve growth factor is critical for cardiac sensory innervation and rescues neuropathy in diabetic hearts. *Circulation* **114**, 2351-2363.
Ieda, M., Kanazawa, H., Kimura, K., Hattori, F., Ieda, Y., Taniguchi, M., Lee, J. K., Matsumura, K., Tomita, Y., Miyoshi, S. et al. (2007). Sema3a maintains normal heart rhythm through sympathetic innervation patterning. *Nat. Med.* **13**, 604-612.
Kayalar, N., Burkhart, H. M., Dearani, J. A., Cetta, F. and Schaff, H. V. (2009). Congenital coronary anomalies and surgical treatment. *Congenit. Heart Dis.* **4**, 239-251.
Kuruvilla, R., Zweifel, L. S., Glebova, N. O., Lonze, B. E., Valdez, G., Ye, H. and Ginty, D. D. (2004). A neurotrophin signaling cascade coordinates sympathetic neuron development through differential control of TrkA trafficking and retrograde signaling. *Cell* **118**, 243-255.
Larrivée, B., Freitas, C., Suchting, S., Brunet, I. and Eichmann, A. (2009). Guidance of vascular development: lessons from the nervous system. *Circ. Res.* **104**, 428-441.
Lavine, K. J. and Ornitz, D. M. (2009). Shared circuitry: developmental signaling cascades regulate both embryonic and adult coronary vasculature. *Circ. Res.* **104**, 159-169.
Lavine, K. J., Long, F., Choi, K., Smith, C. and Ornitz, D. M. (2008). Hedgehog signaling to distinct cell types differentially regulates coronary artery and vein development. *Development* **135**, 3161-3171.
Levi-Montalcini, R. (1987). The nerve growth factor 35 years later. *Science* **237**, 1154-1162.
Luff, S. E. (1996). Ultrastructure of sympathetic axons and their structural relationship with vascular smooth muscle. *Anat. Embryol. (Berl.)* **193**, 515-531.
Makita, T., Sucov, H. M., Gariepy, C. E., Yanagisawa, M. and Ginty, D. D. (2008). Endothelins are vascular-derived axonal guidance cues for developing sympathetic neurons. *Nature* **452**, 759-763.
Mikawa, T. and Fischman, D. A. (1992). Retroviral analysis of cardiac morphogenesis: discontinuous formation of coronary vessels. *Proc. Natl. Acad. Sci. USA* **89**, 9504-9508.
Mukouyama, Y. S., Shin, D., Britsch, S., Taniguchi, M. and Anderson, D. J. (2002). Sensory nerves determine the pattern of arterial differentiation and blood vessel branching in the skin. *Cell* **109**, 693-705.
Pattyn, A., Morin, X., Cremer, H., Goridis, C. and Brunet, J. F. (1999). The homeobox gene Phox2b is essential for the development of autonomic neural crest derivatives. *Nature* **399**, 366-370.
Red-Horse, K., Ueno, H., Weissman, I. L. and Krasnow, M. A. (2010). Coronary arteries form by developmental reprogramming of venous cells. *Nature* **464**, 549-553.
Rhee, D. Y., Zhao, X. Q., Francis, R. J., Huang, G. Y., Mably, J. D. and Lo, C. W. (2009). Connexin 43 regulates epicardial cell polarity and migration in coronary vascular development. *Development* **136**, 3185-3193.
Tallini, Y. N., Shui, B., Greene, K. S., Deng, K. Y., Doran, R., Fisher, P. J., Zipfel, W. and Kotlikoff, M. I. (2006). BAC transgenic mice express enhanced green fluorescent protein in central and peripheral cholinergic neurons. *Physiol. Genomics* **27**, 391-397.
Walker, D. L., Vacha, S. J., Kirby, M. L. and Lo, C. W. (2005). Connexin43 deficiency causes dysregulation of coronary vasculogenesis. *Dev. Biol.* **284**, 479-498.
Wang, H. U., Chen, Z. F. and Anderson, D. J. (1998). Molecular distinction and angiogenic interaction between embryonic arteries and veins revealed by ephrin-B2 and its receptor Eph-B4. *Cell* **93**, 741-753.
Zamora, M., Männer, J. and Ruiz-Lozano, P. (2007). Epicardium-derived progenitor cells require beta-catenin for coronary artery formation. *Proc. Natl. Acad. Sci. USA* **104**, 18109-18114.
Zhang, J. C., Kim, S., Helmke, B. P., Yu, W. W., Du, K. L., Lu, M. M., Strobeck, M., Yu, Q. and Parmacek, M. S. (2001). Analysis of SM22alpha-deficient mice reveals unanticipated insights into smooth muscle cell differentiation and function. *Mol. Cell. Biol.* **21**, 1336-1344.
Zhou, B., Ma, Q., Rajagopal, S., Wu, S. M., Domian, I., Rivera-Feliciano, J., Jiang, D., von Gise, A., Ikeda, S., Chien, K. R. et al. (2008). Epicardial progenitors contribute to the cardiomyocyte lineage in the developing heart. *Nature* **454**, 109-113.